Med Chem Res (2013) 22:5431–5441
DOI 10.1007/s00044-013-0496-5

MEDICINAL CHEMISTRY RESEARCH

ORIGINAL RESEARCH

Study of binding of pyridoacridine alkaloids on topoisomerase II using in silico tools

Ashwani Kumar · Sunil Kumar · Sandeep Jain · Parvin Kumar · Ruchika Goyal

Received: 22 March 2012 / Accepted: 15 January 2013 / Published online: 27 February 2013

Abstract In this research, the pyridoacridines alkaloids have been docked computationally to the active site of Topoisomerase II using four PDB structures (1PVG, 1QZR, 1AJ6 and 1ZXM). iGEMDOCK 2.1, AutoDock Vina 1.1.2 and AutoDock 4.2.1 were employed to perform the automated molecular docking. The results of docking studies generated docking scores and IC_{50} values. Moreover, 3D pictures of ligand enzyme complexes afforded valuable data regarding the binding orientation of each inhibitor in the active site of Topoisomerase II.

Keywords Topoisomerase II · Pyridoacridine alkaloids · Molecular docking · iGEMDOCK · AutoDock Vina · AutoDock

Introduction

Topoisomerases are the nuclear enzymes that induce transient breaks in the DNA. There are two types of Topoisomerases—Topoisomerase I and Topoisomerase II. Topoisomerase I seems not to be as essential as Topoisomerase II for the survival of eukaryotic cells (Caroline and Katherine, 1998; Smiley *et al*., 2007; Thakur, 2011). So, it has been reviewed that most attention has been paid on the drugs acting on Topoisomerase II (Molinski, 1993; Hangstler *et al*., 2002). This enzyme plays a critical role in transcription and replication of DNA (Cortés *et al*., 2003; Kumar and Rawat, 2011), and also maintains the DNA topology, distangles knotted DNA, maintains correct chromosome condensation, decondensation, and segregation (Sorensen *et al*., 1996; Wang, 1998). It has been well-reviewed that it is a validated target of various antineoplastic drugs like anthracyclines (doxorubicin, daunorubicin), epipodophyllotoxins but are limited by their tumor resistance mechanism, side effects profile and also by their sensitivity to P-gp receptor mediated efflux. Now it is well-established that several antineoplastic agents those act through intercalation also acts on Topoisomerase II (Lee, 1996, Hawtin *et al*., 2010).

Literature of traditionally occurring medicines shows that natural products have very wide role and they are valuable source for new drug discovery (Fabricant and Farnsworth, 2001; Butler, 2004; Harvey, 2008). Crystallographic data based molecular modeling has been used to aid the design of synthetic analogs of natural products (Corbett and Berger, 2004; Huang *et al*., 2011; Nematollahi *et al*., 2011). There are so many compounds possessing pyridoacridine skeleton having anti-HIV activity, Ca^{2+} releasing activity, metal chelating property, DNA intercalating activity, and Topoisomerase II inhibition property (Bhakuni and Rawat, 2005; Kumar and Rawat, 2011). Pyridoacridines are colored marine alkaloids having 7H- pyrido [2, 3, 4-kl] acridine skeleton (Molinski, 1993; Skyler and Heathcock, 2002) (Fig. 1).

The tetracyclic members of this class are archetypical pyridoacridines. Nine cytotoxic tetracyclic alkaloids, Cystodytins A-I have been identified from yellow tunicate *Cystodytes dellechiajei*. Cystodytins A and Cystodytins F are shown in Fig. 2a, b Cystodytins A–C are the first

A. Kumar · S. Kumar · S. Jain · R. Goyal (✉)
Drug Discovery and Research Laboratory, Department of Pharmaceutical Sciences, Guru Jambheshwar University of Science and Technology, Hisar 125001, India
e-mail: ruchikagoyal1@gmail.com

P. Kumar
Department of Chemistry, Kurukshetra University, Kurukshetra, India

Fig. 1 General structure of pyridoacridines

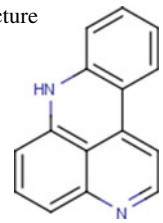

member of this class (Bontemps *et al*., 2010; Kumar and Rawat 2011). Cystodytin A–C and Varamine A and C (Fig. 2c, d) have been found to be cytotoxic against L-1210 (Kumar and Rawat, 2011).

A novel pentacyclic alkaloid, ascididemin isolated from brown colored tunicate *Didemnum* sp. has been found to be cytotoxic against L-1210 marine leukemia cells (Kumar and Rawat, 2011). Ascididemin and its isomers also exhibited cytotoxicity against U-87MG, U-373MG, T-47D, MCF-7, HCT-15, A-549, A-427, T-24, and J-82 cell lines (Matsumoto *et al*., 2003; Bhakuni and Rawat, 2005) (Fig. 2e, f).

Cyclodercitin, a hexacyclic alkaloid shown in Fig. 2g, obtained from the extracts of a deep violet sponge *Dercitus* sp. inhibits the proliferation of P-388 murine leukemia cells. It has also been reviewed that Eilatin, a heptacyclic pyridoacridine exhibits cytotoxic activity against HCT cell line (Stanslas *et al*., 2000; Kumar and Rawat, 2011). Eilatin octacyclic analog does not show any activity against HT-29 (Fig. 2h).

Therefore, it can be said that mostly all pyridoacridines have an immense role as anticancer agents. It is supposed that these compounds show anticancer effect due to inhibition of Topoisomerase II (Dias *et al*., 2005; Sanchez-Carrasco *et al*., 2008; Cragg *et al*., 2009). So, we report herein the study describing binding of pyridoacridine alkaloids against Topoisomerase II, which has been carried out by molecular docking investigations.

Fig. 2 **a–h** Examples of various novel pyridoacridine alkaloids

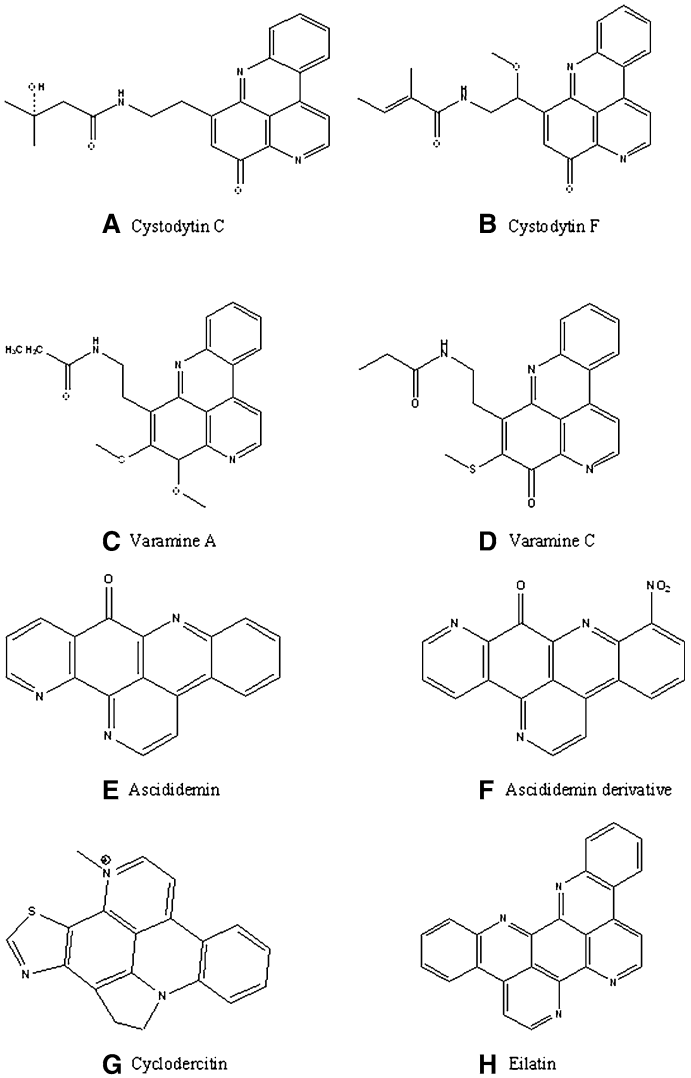

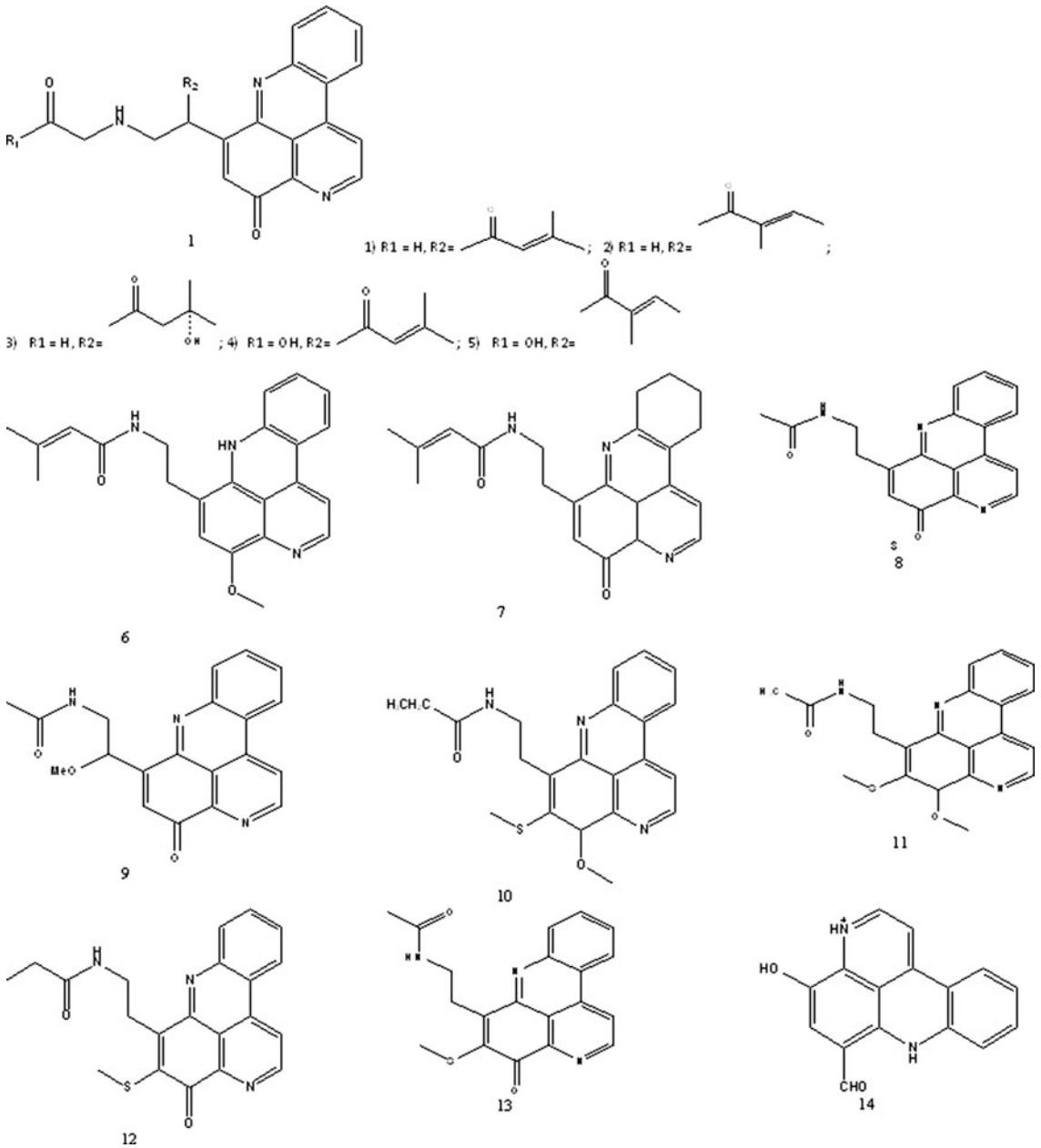

Fig. 3 **a–c** Structures of various pyridoacridine ligands

Computational details

Regarding this issue the crystal structures of Topoisomerase II were obtained from the Brookhaven Protein Data Bank http://www.rcsb.org/pdb (PDB entry: 1ZXM, 1PVG, 1AJ6 and 1QZR). To carry out docking studies, the 2D structures of various pyridoacridine ligands (Kumar and Rawat, 2011; Menna *et al*., 2011) were drawn (Fig. 3a–c) and these were converted into 3D and their energy was minimized using MM2 method with RMS gradient of 0.1 centers. These compounds were saved in mdl mol and pdb files for further use. Docking studies were carried out by *i*GEMDOCK 2.1, AutoDock Vina 1.1.2, and AutoDock 4.2.1 programs. In order to perform the task, the various interactions formed by docked ligands were observed.

To insure that the ligand orientation and the position obtained from the docking studies were likely to represent valid and reasonable binding modes of the inhibitors, docking of co-crystallized ligands were carried out for all protein structures (1PVG, 1QZR, 1AJ6, and 1ZXM). The ligand conformation found in the crystal structure, was extracted and docked back to the corresponding binding pocket. Results of control docking showed the optimal orientation of the docked inhibitor, close to that of the

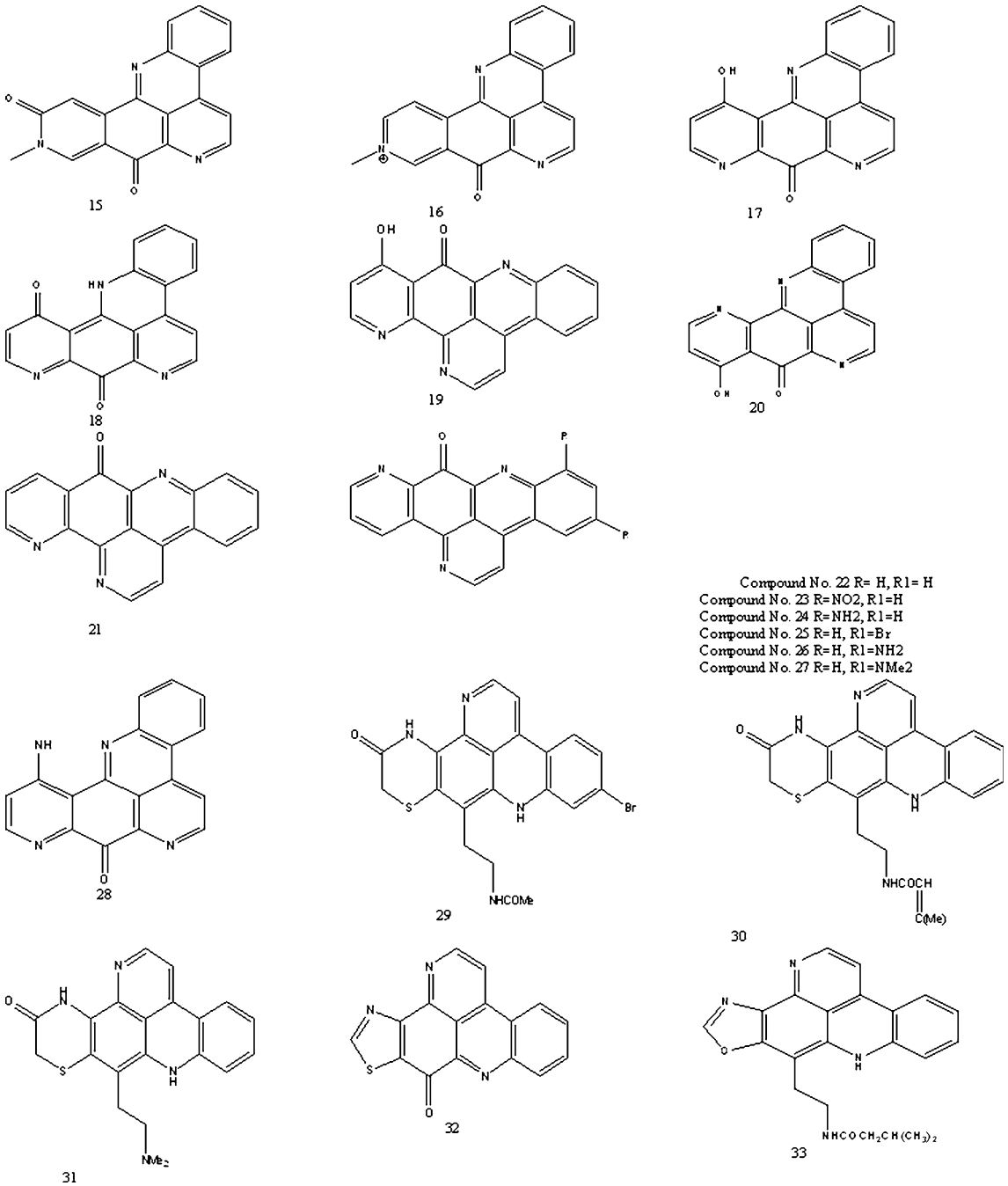

Fig. 3 continued

original orientation found in the crystal as shown in Fig. 4. The RMS deviation of less than 0.2 Å between the docked and crystal ligand coordinates indicate very good alignment of the experimental and calculated positions.

In *i*GEMDOCK (*i*GEMDOCK ver. 2.1), drug screening was used as default settings with population size 200, 70 generations, and 3 numbers of solutions. *i*GEMDOCK scoring function was chosen along with ligand intra energy with hydrophobic and electrostatic preference both as 1.

Finally, ranking of compounds were done by pharmacological energy i.e.,

$$E_{\text{pharma}} = E_{\text{GEMDOCK}} + E(E)_{\text{pharma}} + 2E(H)_{\text{pharma}} + 0.5E(V)_{\text{pharma}};$$

whereas, E_{GEMDOCK} is the docked energy of *i*GEMDOCK and $E(E)_{\text{pharma}}$, $E(H)_{\text{pharma}}$, and $E(V)_{\text{pharma}}$ are the pharmacological scores of electrostatics, hydrogen-bonding, and vdW interactions (Hsu *et al*., 2011), respectively.

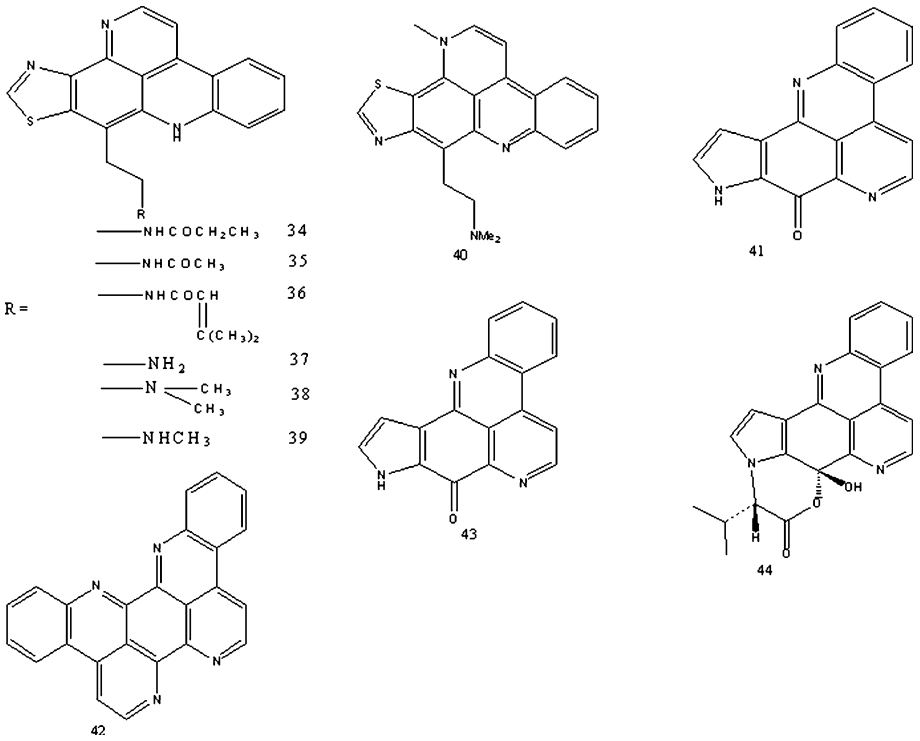

Fig. 3 continued

Fig. 4 ANP docked molecule (1PVG) (UCSF Chimera ver. 1.5.3)

For AutoDock Vina (Trott and Olson, 2010), ligands were removed from pdb files and protein molecules were prepared by deleting solvent molecules and non-complex ions. Incomplete side chains were replaced using Dun Brack Rotamer library (Dunbrack, 2002). Hydrogens were added and gasteiger charges were calculated using Antechamber. The prepared files were saved in pdb format and used for further studies. Similarly, ligand files were prepared in pdb format with explicit hydrogen addition. All pdb files were transformed into pdbqt format. Grid center was placed on the active site. The sizes and centers of grid box are given in Table 1.

Exhaustiveness which influences the thoroughness of the global search algorithm was set to be 8. Then, finally docking results were viewed using PDB and PDBQT files.

Table 1 Size and center of grid box

PDB	1ZXM	1PVG	1QZR	1AJ6
Center x	36.9740811016	27.8898113151	24.8441590144	60.0523309934
Center y	−2.86672433285	51.7398051666	48.6722229202	−1.52863290342
Center z	30.7087891051	36.4549667271	37.3837898727	43.5987509439
Size x	27.9805030584	25.3277518132	22.1797711593	23.961169406
Size y	25.0942215581	20.8002295979	22.383894233	27.3153928938
Size z	29.6831974931	21.9755034483	22.8556267793	21.9298182199

Table 2 Grid center and number of points

PDB	1ZXM	1PVG	1QZR	1AJ6
Grid center x	37.6690	19.6211	21.2699	58.4790
Grid center y	−1.8213	49.1703	47.1409	1.7504
Grid center z	36.9128	38.3176	38.4511	42.3218
No. of points x	43	43	47	38
No. of points y	38	37	50	39
No. of points z	51	41	46	41

To gain better insight, AutoDock (Morris *et al*., 1999) was also employed to dock the selected pyridoacridine ligands. The prepared ligand files were transformed to pdbqt format, non-polar hydrogens were merged and charges were defined. The grid calculations were setup and maps were calculated using the program AutoGrid. The Grid maps were centered on the ligand binding site and dimensions were noted. The grid spacing was 0.3750 Å and the default AutoDock parameter settings were used for

Table 3 Docking scores for PDB 1PVG and 1QZR

Compound no.	1PVG			1QZR		
	*i*GEMDOCK	AutoDock Vina	AutoDock	*i*GEMDOCK	AutoDock Vina	AutoDock
1	−134.4	−9.9	−8.35	−127.1	−9.6	−5.61
2	−134.2	−9.7	−7.42	−110.7	−9.6	−7.48
3	−120.8	−9.7	−6.32	−99.6	−10	−7.49
4	−144.8	−10.1	−7.08	−112.5	−9.7	−6.12
5	−154.7	−10.6	–	−117.2	−10.7	−7.25
6	−133.5	−8	−4.7	−146.2	−8.7	24.27
7	−117.1	−8.2	−4.67	−145.7	−8.8	52.76
8	−133.1	−9.9	−7.62	−109.2	−9.6	−8.29
9	−102.7	−9.8	−7.97	−162.1	−9.9	−7.68
10	−128.8	−10	−7.68	−165.6	−9.5	−9.03
11	−119.4	−10	−7.06	−145	−8.3	−7.81
12	−117.4	−9.4	−8.36	−145.9	−8.6	−5.95
13	−103.4	−8.9	−6.54	−154.7	−8.1	−7.08
14	−103.6	−9.3	−7.74	−103.7	−8.9	−7.16
19	−88	−9.1	−7.44	−134.8	−9.2	−8.13
20	−123.4	−9.1	−7.02	−155.3	−9.1	−7.79
21	−103.2	−9.6	−7.59	−102.5	−9.9	−8.11
22	−83.9	−10.1	−7.25	−96.2	−9.2	−7.94
23	−102.3	−10.1	−7.79	−90.4	−10.2	−8.07
24	−78.1	−10.3	−6.99	−128.7	−10	−8.15
25	−114.7	−10.3	−7.01	−128.6	−10	−8.16
26	−90.3	−9.2	−7.02	−128	−10.1	−8.11
27	−80.3	−10.5	−7.08	−109.2	−10.6	−8.22
28	−88.5	−9.1	−6.77	−127	−9.9	−7.73
29	−85.8	−9	−6.84	−140.4	−9.5	−7
30	−94.5	−8.1	−3.03	−93.9	−7.7	−7.64
31	−115.3	−8.9	−7.58	−135.6	−9	−7.56
32	−88.8	−8	−6.62	−125.5	−7.9	−7.3
33	−89	−8.9	−6.79	−133.5	−9.3	−7.43
34	−114	−6.8	−6.2	−99.5	−7.3	−6.44
35	−88.4	−10.4	−7.61	−128.2	−9.9	−8.82
36	−100.1	−7	−7.79	−138	−8.5	−5.89
37	−144.8	−9.8	−7.78	−162.1	−9.6	−8.81
38	−93.9	−10	−7.19	−143.9	−9.7	−7.27
39	−121.5	−9	−6.16	−140.3	−8.9	−6.31
40	−115.9	−7	−6.75	−135.2	−7.1	−6.26
41	−107.1	−9.1	−6.56	−130.2	−9.8	−7.31

Table 3 continued

Compound no.	1PVG			1QZR		
	*i*GEMDOCK	AutoDock Vina	AutoDock	*i*GEMDOCK	AutoDock Vina	AutoDock
42	−87.3	−8.9	−6.75	−131.3	−9.9	−7.33
43	−130.9	−9.3	−7.38	−162	−9.1	−8.77
44	−127.9	−9.3	−7.6	−153.7	−9.6	−7
Ligand	−91.7	−11.4	–	−106.1	−11.3	–

Table 4 Docking scores for PDB 1AJ6 and 1ZXM

Compound no.	1AJ6			1ZXM		
	*i*GEMDOCK	AutoDock Vina	AutoDock	*i*GEMDOCK	AutoDock Vina	AutoDock
1	−174.5	−8.6	−5.26	−134.5	−9.7	−8.01
2	−171.2	−8.5	−5.96	−131.2	−10.7	−9.62
3	−177.7	−8.5	−5.8	−154.1	−10.7	−8.74
4	−188.1	−8.6	−5.9	−144.4	−10.5	−9.21
5	−161.3	−8.5	−6.4	−165.1	−11.1	−8.64
6	−174.2	−6.8	−6.1	−118.6	−8.7	0.76
7	−179.1	−5.9	–	−175.2	−8.9	−4.6
8	−182.4	−8.2	−5.48	−143.1	−9.6	−8.83
9	−168.9	−8.3	−6.23	−152.2	−10.5	−9.38
10	−159.3	−8.4	−6.28	−136.6	−10.7	−9.11
11	−180.1	−9.5	−6.88	−154.4	−9.2	−8.14
12	−159.3	−7.3	−5.33	−144.5	−9.2	−9.03
13	−137.6	−7.9	−4.39	−144.4	−10.3	−8.72
14	−155.9	−6.8	−5.91	−141.8	−9.1	−8.87
19	−169.8	−8.3	−6.13	–	−11	–
20	−184.2	−4.2	0.21	–	–	−3.05
21	−153.2	−8.5	−6.15	−120.4	−9.3	−7.63
22	−152.7	−8.6	−5.78	−132.3	−11	−7.81
23	−148.1	−8.4	−5.65	–	−9.9	−7.52
24	−143.2	−8.3	−5.57	−132	−10.8	−8.1
25	−161.2	−9	−5.72	−151.9	−10.5	−7.17
26	−160.9	−9	−5.73	−152.2	−10.5	−7.17
27	−168	−9.1	−7.45	−146.2	−10	−7.1
28	−155.1	−7.7	−6.25	−116.4	−10.2	−7.13
29	−161.3	−9.3	−7.59	−129.1	−9.6	−6.91
30	−161.4	−9.2	−7.11	−126.7	−9.6	−7
31	−169.3	−3.4	−4.57	−131.2	−9	−3.59
32	−167.9	−8.6	−6.18	−114	−9.3	−7.97
33	−159.2	−8.9	−6.53	−123.3	−8.7	−7.09
34	−165.9	−8.8	−6.67	−134.1	−9.6	-6.9
35	−161.6	−8.7	−6.07	−130	−7.7	−6.57
36	−162.4	−8.8	−6.29	−137.9	−10.3	−7.52
37	−185.7	−8.1	−5.15	−138.8	−8.1	−8.26
38	−142.9	−9.1	−4.91	–	–	−8.68
39	−142.8	−8.7	−4.84	−154.8	−8.7	−8.9
40	−177.6	−8.3	−5.11	−126.7	−7.5	−7.26

Table 4 continued

Compound no.	1AJ6			1ZXM		
	*i*GEMDOCK	AutoDock Vina	AutoDock	*i*GEMDOCK	AutoDock Vina	AutoDock
41	−177.2	−7.1	−4.45	−132.4	−7.5	−7.41
42	−159.9	−8.2	−7.55	–	–	−6.67
43	−159.7	−8.2	−7.27	−118.3	−9	−6.75
44	−178.3	−8.6	−5.83	−145.7	−10.7	−8.74
Ligand	−133.5	−6.5	25.8	−184.8	−11.3	–

Table 5 Predicted IC_{50} values, experimental IC_{50} values of some pyridoacridines

Compound no.	Experimental IC_{50} (μM)	Predicted IC_{50} (μM)
1	0.592	79.77
2	0.592	3.29
3	0.639	3.24
4	1.1	20.68
5	3.749	4.82
6	0.125	422.61
12	0.076	43.18
13	0.132	6.49
21	1.376	2.08

docking. The grid centers and number of points are shown in Table 2. All docking runs were performed using Lamarckian genetic algorithm and the obtained Dock scores were reported in kcal/mol. The docking protocol utilized in the study consisted of 10 independent GA runs, using an initial population of 150 randomly placed individuals, a maximum number of 250,000 energy evaluation, mutation rate of 0.02, a crossover rate of 0.80, and an elitism value of 1.

Results and discussion

Topoisomerase II inhibitors with varying structural features and inhibition constants were selected from the literature and were docked into the catalytic site of Topoisomerase II. Dock runs of pyridoacridine ligands on protein 1ZXM, 1PVG, 1QZR, and 1AJ6 using *i*GEMDOCK, AutoDock, and Auto Dock Vina resulted in few best compounds that were evaluated based on their binding compatibility [docked energy (kcal/mol)] with the receptor. The results of docking experiments with these inhibitors are summarized in Tables 3 and 4. These results are mainly evaluated by structure analysis of the docked complexes.

The IC_{50} values (μM) were recorded for the lowest binding energy mode by AutoDock Tools (AutoDock Tools ver. 1.5.6 rc2). The calculated IC_{50} values could not be correlated with the experimental values as the later values are not from direct inhibition of Topoisomerase II. The predicted IC_{50} value and experimental IC_{50} values are shown in Table 5.

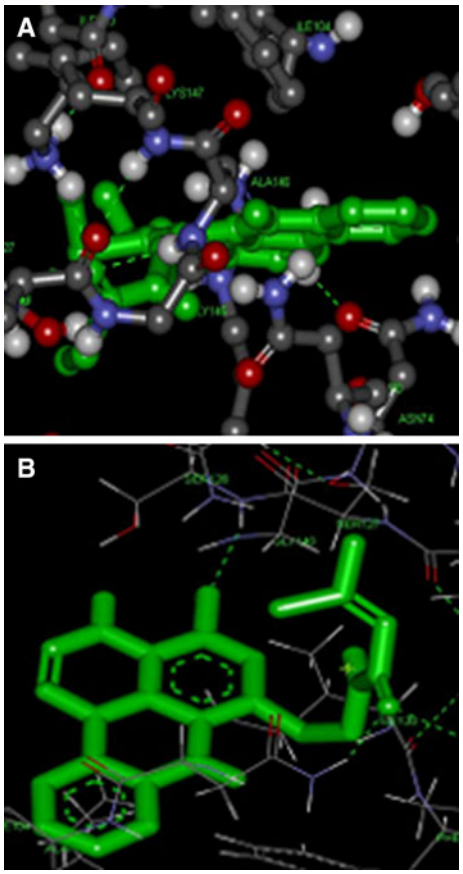

Fig. 5 **a**, **b** H-bonding interactions of compound no. **16** and **12** with Topoisomerase II (1QZR and 1PVG)

Hydrogen-bonding interactions of compounds were visualized using Discovery Studio Visualizer as shown in Fig. 5. Compound no. **6** and **7** are having hydroxyl group which showed hydrogen-bonding interactions with SER 149, ASN 150, ALA 167, and LYS 168. Compound No. **56** was sandwiched in between ARG 76 and ILE 78 through Sigma-Pi stacking interactions (Fig. 6a). Docked poses of some compounds showing hydrogen-bonding interaction

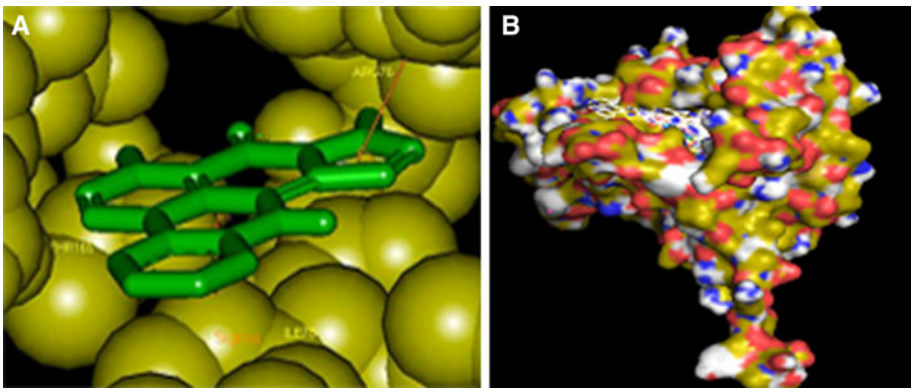

Fig. 6 **a** The Sigma–Pi interactions of compound no. **56** with Topoisomerase II (1AJ6) and **b** Surface diagram of all docked molecules into Topoisomerase II (1QZR)

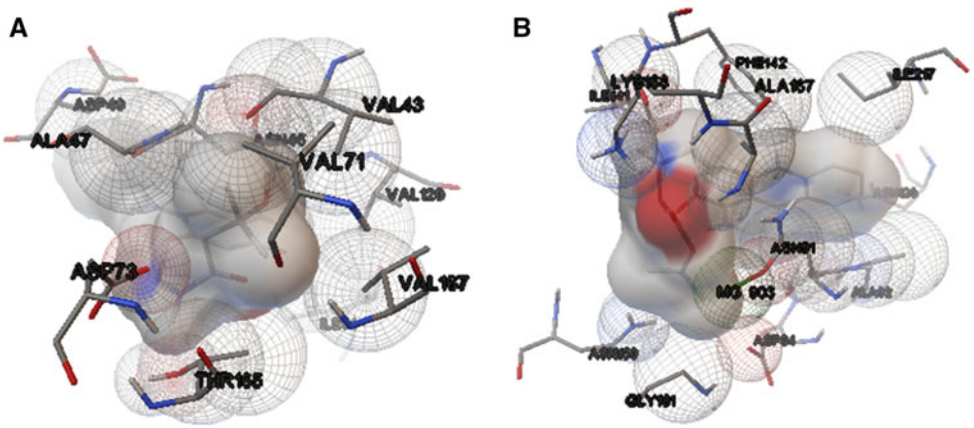

Fig. 7 **a**, **b)** Docking poses, interaction of compound no. **3** and **5** with Topoisomerase II (1AJ6 and 1ZXM)

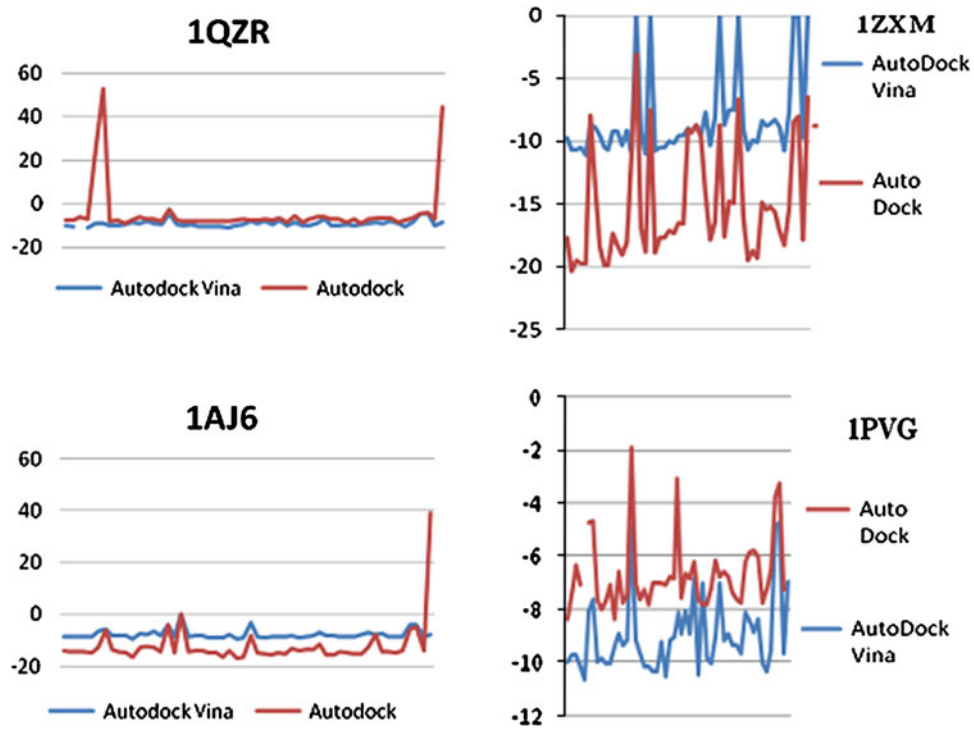

Fig. 8 Graphical representation of docking scores by the two docking programs Autodock and Autodock Vina

and Van der Waal interactions are shown with the help of AutoDock Tools in Fig. 7. Most of the compounds showed hydrogen-bonding interactions with SER 128, SER-149, TYR 165, ALA 167, ILE 120, ARG 76, and Vander Waal interactions with ASN-91, ALA-92, ASN-95, ARG-98, ILE-125, ILE-141, PHE-142, and THR-215. Surface

diagram of all the ligands docked on PDB structure 1QZR is shown in Fig. 6b (PyMol, 2008).

The compound no. **11** exhibits a good score with *i*GEMDOCK but not with other two programs and its predicted IC_{50} value is found to be very high as compared to experimental value which may be due to some physical properties of the molecule and/or some another mechanism responsible for anticancer activity. For molecules containing lesser bulkier groups attached to the ring, good scores were given by all the three programs.

The correlation of docking scores by the two programs AutoDock and AutoDock Vina is shown graphically in Fig. 8. It can be seen that most of the compounds shows a correlation in their docking scores e.g., Compound no. **14** and **15** but there are also some compounds like **46** and **47**, which do not correlate in their docking scores. Almost all the compounds except **11**, **22**, and **35** gave better score then bounded ligand with AutoDock Vina and AutoDock in case of PDB 1AJ6. Scores of *i*GEMDOCK could not be correlated with docking scores of other two softwares used.

Conclusion

Docking programs allowed us to estimate the docking scores, binding modes, and inhibition constants for the molecules under study. Almost all the compounds chosen except a few are found to be active against Topoisomerase II. In case of PDB 1AJ6, some ligands showed better fitness even than the co-crystallized ligand. An idealized representation of each ligand that makes every possible potential interaction with the binding site and other data obtained from all three programs *i*GEMDOCK, AutoDock Vina, and AutoDock, conclude that pyridoacridines are successfully docked into the protein binding site. Furthermore, this study will help in designing of novel derivatives of pyridoacridines and in discovery of new chemical entities for anticancer therapy.

References

*i*GEMDOCK (version 2.1) BioXGEM Lab © 2001–2010

AutoDock Tools (version 1.5.6 rc2), Stefano Forte. Molecular Graphics Laboratory, Department of Molecular Biology, The Scripps Research Institute http://mgltools.scripps.edu © (1999–2010)

Bhakuni DS and Rawat DS (2005) Bioactive marine natural products. Springer, New York, ISBN: 1-4020-3472-5

Bontemps N, Bry D, López-Legentil S (2010) Structures and antimicrobial activities of pyridoacridine alkaloids isolated from different chromotypes of the ascidian Cystodytes dellechiajei. J Nat Prod 73:1044–1048

Butler MS (2004) The role of natural product chemistry in drug discovery. J Nat Prod 67:2141–2153. doi:10.1021/np040106y

Caroline AA, Katherine LM (1998) Eukaryotic DNA topoisomerase II β. BioEssays 20:215–226

Corbett KD, Berger JM (2004) Structure, molecular mechanisms, and evolutionary relationships in DNA Topoisomerases. Annu Rev Biophys Biomol Struct 33:95–118. doi:10.1146/annurev.biophys.33.110502.140357

Cortés F, Pastor N, Mateos S, Dominguez I (2003) Roles of DNA topoisomerases in chromosome segregation and mitosis. Mutat Res 543:59–66

Cragg GM, Grothaus PG, Newman DJ (2009) Impact of natural products on developing new anti-cancer agents. Chem Rev 109: 3012–3043

Dias N, Vezin H, Lansiaux A et al (2005) Topoisomerase inhibitors of marine origin and their potential use as anticancer agents. Top Curr Chem 253:89–108. doi:10.1007/b100444

Discovery Studio Visualizer (version 2.5.5.9350), Accelrys Software Inc. © 2005–2009

Dunbrack RL Jr (2002) Rotamer libraries in the 21st century. Curr Opin Struct Biol 12:431–440

Fabricant DS, Farnsworth NR (2001) The value of plants used in traditional medicine for drug discovery. Environ Health Perspect 109:69–75

Hangstler JG, Heimerdinger CK, Schiffer IB et al (2002) Dietary Topoisomerase II- poisons contribution of soy products to infant leukaemia. EXCLI J 1:8–14

Harvey AL (2008) Natural products in drug discovery. Drug Discov Today 13:894–3426. doi:10.1016/j.drudis.2008.07.004

Hawtin RE, Stockett DE, Byl JAW et al (2010) Voreloxin is an anticancer quinolone derivative that intercalates DNA and poisons topoisomerase II. PLOS one 5:1–3

Hsu KC, Chen YF, Lin SR, Yang JM (2011) *i*GEMDOCK: a graphical environment of enhancing GEMDOCK using pharmacological interactions and post-screening analysis. BMC Bioinformatics 12:1–11

Huang XY, Shan ZJ, Zhai HL et al (2011) Molecular design of anticancer drug leads based on three-dimensional quantitative structure_activity. J Chem Inf Model 51:1999–2006

Kumar D, Rawat DS (2011) Marine natural alkaloids as anticancer agents. In: Opportunity challenge and scope of natural products in medicinal chemistry, pp 213–268. ISBN: 978-81-308-0448-4

Lee KH (1996) Anticancer drug design based on plant-derived natural products. J Biomed Sci 6:236–250

Matsumoto SS, Biggs J, Copp BR (2003) Mechanism of ascidiidemin-induced cytotoxicity. Chem Res Toxicol 16:113–122

Menna M, Fattorusso E, Imperatore C (2011) Alkaloids from marine ascidians. Molecules 16:8694–8732. doi:10.3390/molecules16108694

Molinski TF (1993) Marine pyridoacridine alkaloids: structure, synthesis and biological chemistry. Chem Rev 93:1825–1838

Morris GM, Goodshell DS, Huey R, Hart WE, Halliday RS, Belew RK, Olson AJ, Autodock (1999) (version 4.2.1), Molecular Graphics Laboratory, Department of Molecular Biology, The Scripps Research Institutes, http://www.scripps.edu/pub/olson-web/doc/Autodock/), La Jolla, CA, USA

Nematollahi A, Aminimoghadamfarouj N, Wiart C (2011) Design and Modeling Studies on Liriodenine derivatives as novel topoisomerase II Inhibitors. Int J Chem Tech Res 3:1622–1627

PyMol (TM) (2008) Evaluation Product Delano Scientific LLC. http://www.pymol.org/funding.html © 2008

Sanchez-Carrasco S, Delcros JG, Moya-Garcia AA et al (2008) Study by optical Spectroscopy and molecular dynamics of the interaction of acridine-spermine conjugate with DNA. Biophys Chem 133:54–65. doi:10.1016/j.bpc.2007.12.003

Skyler D, Heathcock CH (2002) The pyridoacridine family tree: a useful scheme for designing synthesis and predicting undiscovered natural products. J Nat Prod 65:1573–1581

Smiley RD, Collins TRL, Hammes GG, Hsieh TS (2007) Single-molecule measurements of the opening and closing of the DNA gate by eukaryotic topoisomerase II. PNAS 104:4840–4845

Sorensen BS, Sinding J, Andersen AH, Alsner J, Jensen PB, Westergaard O (1996) Mode of action of topoisomerase II targeting agents at a specific DNA sequence. Uncoupling the DNA binding, cleavage and relegation events. J Mol Biol 228:778–786

Stanslas J, Hagan DJ, Ellis MJ et al (2000) Antitumor polycyclic acridines. 7.1 synthesis and biological properties of DNA affinic tetra- and pentacyclic acridines. J Med Chem 43:1563–1572

Thakur DS (2011) Topoisomerase II Inhibitors in cancer treatment. IJPSN 3:1173–1181

Trott O, Olson AJ (2010) AutoDock Vina: improving the speed and accuracy of docking with a new scoring function, efficient optimization and multithreading. J Comput Chem 31:455–461

UCSF Chimera (version 1.5.3) by the Regents of the University of California © 2000–2011

Wang JC (1998) Moving one DNA double helix through another by a type II DNA topoisomerase: the story of a simple molecular machine. Q Rev Biophys 31(2):107–144